

Clarification numérique en imagerie des sphéroïdes

Ali AHMAD^{1,2}, Saba GOODARZI³, Carole FRINDEL², Gaëlle RÉCHER⁴, Charlotte RIVIÈRE³, David ROUSSEAU^{2,*}

¹Université Lyon 1, Insa de Lyon, CREATIS, CNRS UMR 5220 - INSERM U1206, Villeurbanne, 69100, France

²Université d'Angers, LARIS, UMR INRAe IRHS, 62 Avenue Notre Dame du Lac, 49000 Angers, France

³Univ Lyon, Université Claude Bernard Lyon 1, CNRS UMR-5306, Institut Lumière Matière, F-69622, Villeurbanne, 69100, France

⁴BioImaging & OptoFluidics, LP2N, CNRS UMR5298, IOGS, Université de Bordeaux, Talence, F-33400, France

david.rousseau@univ-angers.fr

Résumé – Dans les sciences de la vie, on s'intéresse de plus en plus aux modèles de culture 3D pour mieux reproduire l'environnement 3D rencontré *in vivo*. L'imagerie de ces modèles de culture 3D est essentielle pour la découverte de médicaments, mais elle doit relever plusieurs défis avant d'être largement utilisée. L'examen microscopique profond de ces modèles cellulaires 3D est confronté au défi de la pénétration de la lumière dans les tissus biologiques opaques. Pour surmonter cette limitation, diverses techniques de clarification ont vu le jour au cours des dernières décennies. Cependant, ces méthodes sont invasives et coûteuses en temps. En nous concentrant sur les sphéroïdes, nous montrons la possibilité de contourner cette étape en étudiant plusieurs stratégies d'apprentissage profond. Nous montrons qu'un transfert de style, notamment le cycleGAN (cGAN), sera capable de compenser la dégradation des images en profondeur, pour une tâche de segmentation des noyaux, en convertissant les images de sphéroïdes non clarifiées au style des images de sphéroïdes clarifiées par le Glycérol.

Abstract – In the life sciences, there is increasing interest in 3D culture models to better replicate the 3D environment encountered *in vivo*. Imaging of these 3D culture models is essential for drug discovery, but faces several challenges before its widespread use. Deep microscopic examination of these 3D cell models faces the challenge of penetrating light deep into opaque biological tissues. To overcome this limitation, various clarification techniques have emerged over the past decades. However, these methods are invasive and time consuming. Focusing on spheroids, we show the possibility to bypass this step by studying several deep learning strategies. We show that a style transfer, namely the cycleGAN (cGAN), will be able to compensate the degradation of the images in depth, for a nuclei segmentation task, by converting the images of unclarified spheroids to the style of the spheroid images clarified by the Glycerol.

1 Introduction

Deep learning is currently revolutionizing computational imaging [1]. Indeed, it allows to overcome constraints on the reconstruction of raw images that can be directly processed by neural networks without having to produce a beautiful image interpretable by a human brain. This revolution also affects another step in imaging with the preparation of samples via contrast or clarification agents. In microscopy in particular, these agents are chemicals very often used to magnify the contrast or to denoise the sample in order to allow a human to interpret the details of interest [2]. However, this step is time consuming and possibly invasive (requiring *ex-vivo* operation or deforming the tissue). The use of neural networks to bypass such step has been demonstrated in histopathology [3]. In the same spirit, aiming at reducing the sample preparation time, we study a new use of neural networks for digitally clearing samples based on deep transfer learning [10] and style transfer strategies [4, 5].

The article is organized as follows. First, the formation, preparation and image acquisition of spheroids chosen here for illustration are given. Then, tools based on deep learning are described. Finally, results regarding the feasibility of digital

clearing are discussed before the conclusion.

2 Material and Methods

We present the details of all the steps described in the graphical abstract of Fig 1.

2.1 Spheroids formation, Immunostaining and Clarification

Colorectal carcinoma cell line HCT-116 were used in this study. HCT-116 spheroids were formed in 24-well plates containing agarose micro-wells in each well (Fig. 1.A) [6]. Cells were seeded in each 24 wells-plate containing microsystems at a density of 1.2×10^5 cells/mL, 1 mL per well. This leads to an initial seeding of 20–30 cells/micro-well. To encourage and accelerate cell aggregation, the 24-well plate was placed under orbital agitation (160 rpm) for 15 min in the incubator at 37°C and 5% CO_2 . After 4 h, the plate was rinsed with fresh medium to remove cells that did not reach the micro-wells. Multicellular Tumor Spheroids (MCTs) are formed within 1 day and are used at Day 5 in this study.

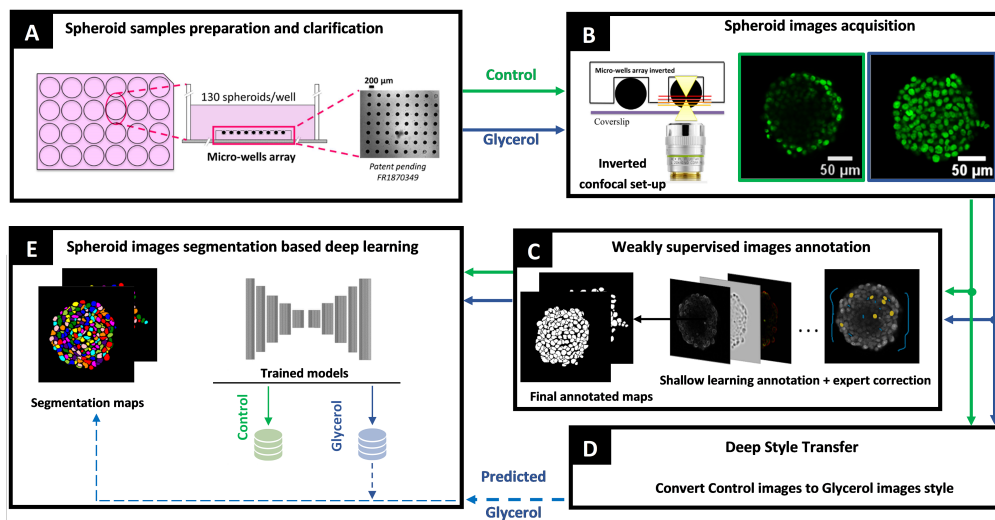


FIGURE 1 – Protocol pipeline : (A) Spheroid samples are cultured in micro-well arrays. Control are the non cleared samples and Glycerol are spheroids cleared with Glycerol. (B) Spheroid images acquired with a confocal microscope. (C) A dataset of images for each condition is annotated using shallow learning and corrected by an expert. (D) Deep learning models were trained to convert the style of Control to Glycerol. (E) Finally, deep learning segmentation models are trained with the control and Glycerol annotated data sets and the segmentation models were used to segment the nuclei.

At day 5, spheroids were washed 3 times with warmed PBS for 5 min, followed by paraformaldehyde fixation (3.7% in PBS) for 20 minutes. All wells were then washed with PBS/3% BSA (3×5 min), permeabilized with 0.5% Triton for 20 min, and rinsed again with PBS/ 3% BSA (3x 5 min). To stain nucleus, NucGreen Dead 488 ReadyProbes Reagent were used. The samples were washed with PBS (1×10 min) and kept protected from light in PBS at 4°C until image acquisition. Such non-cleared samples (Control) were either imaged directly, or further processed with Glycerol clearing method [6].

In order to perform Glycerol clarification, the micro-wells were incubated overnight with a glycerol solution (80% glycerol in PBS (v/v)). The microsystems were then mounted between 2 coverslips, separated by a 1 mm sticky spacer (2 × 0.5 mm-thick Ispacer, SunJin Lab) with 35 µL fresh clearing solution.

2.2 Image acquisition and annotation

A pile of z-stacks images of 512×512 pixels in xy was acquired using a classical confocal set-up. Control and Glycerol images were acquired with Leica SP5 in resonant mode, a 25x water objective lens (NA=0.95) is used with a voxel size of $0.4 \times 0.4 \times 1 \mu\text{m}^3$. A 488 nm line of an Argon Laser was used to detect NucGreen (see Fig. 1.B). The total number of spheroids used in this study is 14 spheroids, imaged before clearing and after Glycerol clearing. These image pairs (Control, Glycerol) were used to train style transfer networks.

Ground truth annotation for nuclei segmentation was performed in semi-automatic way using Ilastik tool [7](Fig. 1.c). 2D frames from the beginning, middle and the end of 3D image

stacks belonging to each clearing condition were selected for exhaustive representation of instances and clearing effects on image depths. Pixel wise classification mode was used then to generate primary segmentation maps. The filters used in the segmentation step were intensity, edge and textural filters with various kernel sizes ranging from 0.7 pixel to 10 pixels in order to represent the smallest and largest details of the transition between the nuclei and the background (36 filters). Finally, a manual correction step produced by an expert was applied to the segmentation maps. The overall amount of annotated 2D images was 57 obtained from 3 spheroids from each clearing condition. Each dataset were then split into 47 to train the segmtnat deep learning models, 5 for validation and 5 for testing.

2.3 Deep learning methods

In this section, we describe the deep learning strategies followed in this study to show the feasibility of numerical clearing of spheroids. They are briefly presented in the following.

DIST We used DIST method proposed in [8]. It is based on the U-Net architecture [9] and consists on predicting the distance maps (\hat{d}) that focus on the center of nuclei instead of probability maps. Therefore, for each pixel $x = (i, j)$ of the annotated spheroid binary image (y), with $y(x) > 0$, we assign a distance transform (D_c) representing the distance to the closest background pixel $x_b = [i_b, j_b]$. Here, we used the Chebyshev distance as proposed in [8]. The training hyper-parameters used are as follows : *batch size* = 1, *epochs* = 50 and the learning rate $lr = 1e^{-3}$. Models training also includes early stop regularization and model checkpoints to save the best weights.

The output function of the Unet architecture was replaced with a ReLU function. The final binary segmentation maps were then obtained by thresholding the distance output maps \hat{d} . Finally, a post-processing step, based on dynamic morphology and the watershed algorithm, was also applied to the predicted maps to improve the final segmentation, as described in [8]. We trained a DIST model for each clearing condition dataset to minimize the mean square error (MSE) loss function. The threshold value β of the distance output maps and h-minima parameters λ of the post processing were empirically optimized on the validation dataset, both in the control and glycerol conditions. They were found as ($\beta_{Control} = 1.1$; $\beta_{Glycerol} = 0.6$) and ($\lambda_{Control} = 2$; $\lambda_{Glycerol} = 1$). The segmentation quality of each model was evaluated on the annotated 5 test images for each condition using the $F1 - score$ as a pixel-wise metric and the Aggregated Jaccard Index (AJI) as an object-wise metrics as used in [8].

Transfer learning We applied the transfer learning methodology [10] in our study to transfer the knowledge gained by the trained DIST model on the Glycerol to the Control dataset. The encoder part of the DIST architecture (Unet) was frozen and we adjusted the decoder weights on the Control data. The same hyper-parameters, as mentioned in the previous section, were used when fine tuning the Control model. This new model was then used to test the ability of knowledge transfer to improve nuclei segmentation on the Control dataset.

Style transfer In order to study the feasibility of converting control spheroid images to Glycerol-cleared spheroid images, we tested two different approaches : the cycleGAN (cGAN) [4] and the pix2pix [5]. The hyper-parameters used to train this models are $batch\ size = 2$, $training\ steps = 38000$ and $lr = 2e - 4$. We trained the models using 4 pairs of 3D spheroid images (Control, Glycerol) containing approximately 380 2D slices for each condition. The models were trained to minimize the loss functions described in [4, 5]. The two trained style transfer models were then applied to 7 3D Control test spheroids and the predicted Glycerol images were finally segmented using the DIST model trained on the glycerol data set.

3 Results and Discussion

Effect of Glycerol clearing on 2D spheroids segmentation

We evaluated the quality of Glycerol clearing based on segmentation metrics. We computed the F1-score and AJI metrics from 5 test images of each clearing condition segmented with their own segmentation model. The Glycerol clearing protocol provides the best segmentation performance with $F1 - score = 0.91 \pm 0.01$ and $AJI = 0.71 \pm 0.02$ better than the Control segmentation with $F1 - score = 0.83 \pm 0.01$ and $AJI = 0.42 \pm 0.05$. This is due to the decrease in image quality of non-cleared spheroids (Control) in deep z (see Fig. 2.A).

Transferability of knowledge from Glycerol to Control To test the transferability of Glycerol knowledge to the control data sets, we performed two different experiments : (i) inference by applying the Glycerol-trained model directly to segment control data ; (ii) fine-tuning the Glycerol model with the control data via Control With TL (Transfer Learning). For this test, the 7 Control test spheroids were used and the segmentation maps of the 7 test Glycerol spheroids were taken as ground truth to compute segmentation metrics. As shown in Fig. 2, the inference strategy (Cyan curves) is able to recompense the segmentation of the Control images in the first half of the spheroids ($z = 0$ to $60\ \mu m$) better than the transfer learning strategy (pink curves). However, both strategies struggle to segment Control images in deep z.

Converting non cleared Control to Glycerol clearing style

In this strategy, we applied style transfer models (cGAN and pix2pix) on the test Control spheroids. The predicted Glycerol images were then segmented using the DIST model pre-trained with the Glycerol data. The results of these experiments are shown in Fig. 2. Both methods provide improved segmentation for all z depths. However, the cGan-based method (brown curves) is more efficient and it overcomes the pix2pix (black curves). This discrepancy between the methods is related to the fact that the cGan method is an unpaired image-to-image translation that does not require a perfect match between the training data (Control, Glycerol), unlike the pix2pix method that requires a pixel-to-pixel correspondance. But however, this perfect match is impossible due to the deformation of spheroids after Glycerol clearing and well rotation during acquisition.

Spheroids digital clearing is feasible

The present studies based on deep learning proves the feasibility of digital clearing. The cGan-based method is well suited to perform such a task, demonstrating the ability of deep learning to relax constraints on spheroid sample preparation. Such a task can be performed on the fly, where style transfer followed by 2D nuclei segmentation requires only about 11.21 seconds for a 113 slices of 118 *mb* spheroid stack computed with a Tesla V100-DGXS-32GB GPU (cGAN=5.53 and DIST=5.68 seconds). The current style transfer model was trained on 2D images with few datasets (only 4 spheroids), such a task could be improved by performing the style transfer with more data and in 3D by taking into account the dependencies between 2D slices. In the present study, we used Glycerol clearing as a reference, other clearing protocols could also be investigated using the same studied pipeline.

4 Conclusion

In this communication, we studied the feasibility of spheroids digital clearing by comparing various deep learning approaches. The best strategy was found by applying the cGan style transfer method which allows to enhance the quality of

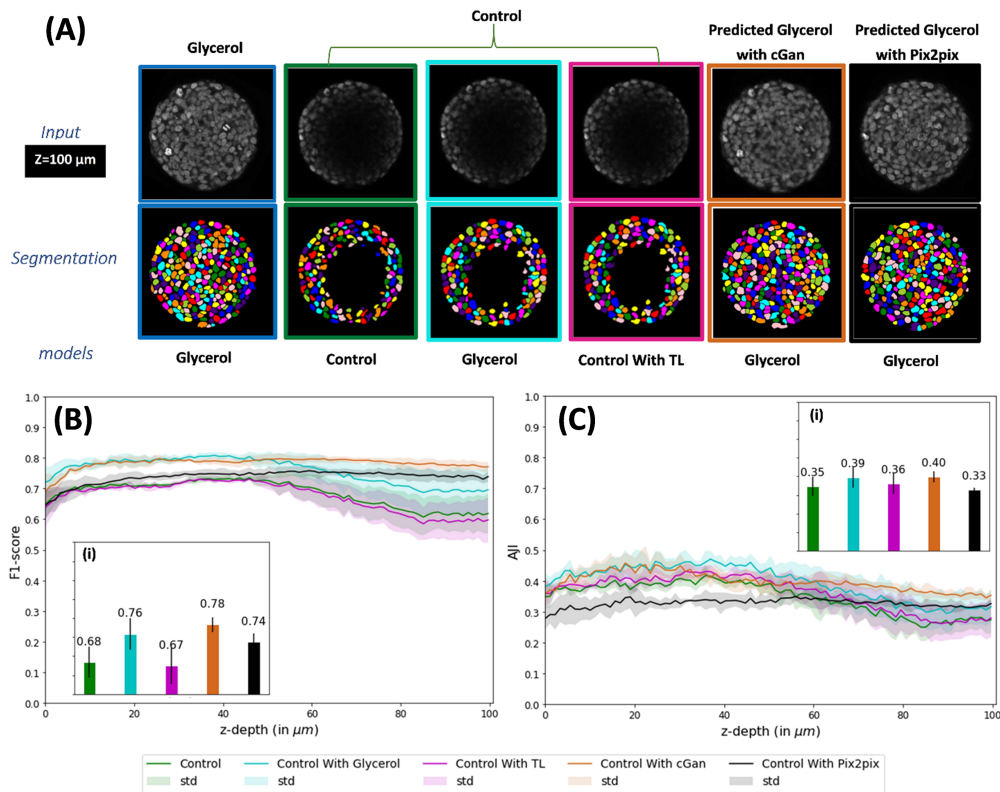


FIGURE 2 – Digital clearing results. **(A)** Illustration of the segmentation results of a control image at $z = 100 \mu\text{m}$ after applying the deep learning strategies. **(B,C)** Mean and standard deviation of segmentation metrics (F1-score, AJI) as a function of z depths (in μm) calculated from 7 test spheroids. **(i)** Histograms showing the total average of the F1-score and AJI measures for each deep learning strategy. Glycerol segmentation maps were used as ground truth to compute the metrics.

uncleared spheroids segmentation and therefore to bypass the preparation step which is invasive and time consuming.

Références

- [1] J. N. Mait, G. W. Euliss, and R. A. Athale, “Computational imaging,” *Advances in Optics and Photonics*, vol. 10, no. 2, pp. 409–483, 2018.
- [2] E. C. Costa, D. N. Silva, A. F. Moreira, and I. J. Correia, “Optical clearing methods : An overview of the techniques used for the imaging of 3d spheroids,” *Biotechnology and bioengineering*, vol. 116, no. 10, pp. 2742–2763, 2019.
- [3] S. Bakas and M. D. Feldman, “Computational staining of unlabelled tissue,” *Nature biomedical engineering*, vol. 3, no. 6, pp. 425–426, 2019.
- [4] J.-Y. Zhu, T. Park, P. Isola, and A. A. Efros, “Unpaired image-to-image translation using cycle-consistent adversarial networks,” in *Proceedings of the IEEE international conference on computer vision*, pp. 2223–2232, 2017.
- [5] P. Isola, J.-Y. Zhu, T. Zhou, and A. A. Efros, “Image-to-image translation with conditional adversarial networks,” in *Proceedings of the IEEE conference on computer vision and pattern recognition*, pp. 1125–1134, 2017.
- [6] S. Goodarzi, A. Prunet, F. Rossetti, G. Bort, O. Tillement, E. Porcel, S. Lacombe, T.-D. Wu, J.-L. Guerquin-Kern, H. Delanoë-Ayari, *et al.*, “Quantifying nanotherapeutic penetration using a hydrogel-based microsystem as a new 3d in vitro platform,” *Lab on a chip*, vol. 21, no. 13, pp. 2495–2510, 2021.
- [7] S. Berg, D. Kutra, T. Kroeger, C. N. Straehle, B. X. Kausler, C. Haubold, M. Schiegg, J. Ales, T. Beier, M. Rudy, *et al.*, “ilastik : interactive machine learning for (bio)image analysis,” *Nature Methods*, pp. 1–7, 2019.
- [8] P. Naylor, M. Laé, F. Reyat, and T. Walter, “Segmentation of nuclei in histopathology images by deep regression of the distance map,” *IEEE transactions on medical imaging*, vol. 38, no. 2, pp. 448–459, 2018.
- [9] O. Ronneberger, P. Fischer, and T. Brox, “U-net : Convolutional networks for biomedical image segmentation,” in *International Conference on Medical image computing and computer-assisted intervention*, pp. 234–241, Springer, 2015.
- [10] S. J. Pan and Q. Yang, “A survey on transfer learning,” *IEEE Transactions on knowledge and data engineering*, vol. 22, no. 10, pp. 1345–1359, 2009.